Recombinant Bovine Heart Mitochondrial F_1-ATPase Inhibitor Protein: Overproduction in *Escherichia coli*, Purification, and Structural Studies†

Gino Van Heeke,*,‡ Lily Deforce,§ Richard A. Schnizer,∥ Regina Shaw,‡ Judy M. Couton,‡ Gerry Shaw,⊥ Pill-Soon Song,§ and Sheldon M. Schuster∥

Protein Expression Laboratory, Interdisciplinary Center for Biotechnology Research, Department of Biochemistry and Molecular Biology, and Department of Neuroscience, University of Florida, Gainesville, Florida 32610, and Department of Chemistry, University of Nebraska—Lincoln, Lincoln, Nebraska 68588-0304

Received June 4, 1993; Revised Manuscript Received July 12, 1993®

ABSTRACT: A synthetic gene coding for the inhibitor protein of bovine heart mitochondrial F_1 adenosine triphosphatase was designed and cloned in *Escherichia coli*. Recombinant F_1-ATPase inhibitor protein was overproduced in *E. coli* and secreted to the periplasmic space. Biologically active recombinant F_1-ATPase inhibitor protein was recovered from the bacterial cells by osmotic shock and was purified to near homogeneity in a single cation-exchange chromatography step. The recombinant inhibitor protein was shown to inhibit bovine mitochondrial F_1-ATPase in a pH-dependent manner, as well as *Saccharomyces cerevisiae* mitochondrial F_1-ATPase. Thorough analysis of the amino acid sequence revealed a potential coiled-coil structure for the C-terminal portion of the protein. Experimental evidence obtained by circular dichroism analyses supports this prediction and suggests F_1I to be a highly stable, mainly α-helical protein which displays C-terminal α-helical coiled-coil intermolecular interaction.

Bovine heart mitochondrial F_1 adenosine triphosphatase (ATPase) inhibitor protein (bmF_1I)[1] is an 84 amino acid protein which inhibits both coupled and uncoupled F_1-ATPase activity, but does not affect the steady-state rate of ATP production during oxidative phosphorylation [Pulman & Monroy, 1963; Schwerzmann & Pedersen, 1981; Frangione *et al.*, 1981; see Schwerzmann and Pedersen (1986) and Rouslin (1991) for reviews]. F_1-ATPase inhibitor proteins with characteristics similar to the bovine protein have been isolated from several other eukaryotic sources including *Saccharomyces cerevisiae* (Hashimoto *et al.*, 1981), *Candida utilis* (Klein et al., 1977), and rat liver mitochondria (Cintron & Pedersen, 1979) as well as from prokaryotes (Smith & Sternweis, 1977) and chloroplasts (Nelson *et al.*, 1972; Nieuwenhuis *et al.*, 1974).

The interaction between F_1 and the inhibitor protein has been partially characterized. The bmF_1I has been shown to bind to the β subunit of F_1 in a stoichiometry of 1 per F_1 complex (Klein *et al.*, 1980, 1981; Wong *et al.*, 1982), so it is likely that inhibition of ATP hydrolysis is mediated through a single β subunit. Current models of the interaction of the inhibitor protein with F_1-ATPase depend on conformational changes in the ATPase complex (Schwerzmann & Pedersen, 1986), the inhibitor protein itself (Panchenko & Vinogradov, 1985; Fujii *et al.*, 1983; Milgrom, 1991, or both. The inhibitor protein can exist in at least two conformations. The active conformation predominates at acidic pH, and the inactive one at basic pH. Protonation of histidine residues has been implicated in the conformational transition of both bovine and yeast inhibitor proteins (Panchenko & Vinogradov, 1985; Fujii *et al.*, 1983). The active form of the inhibitor inactivates F_1 immediately, whereas inhibition by the inactive form takes minutes and is turnover dependent (Schwerzmann & Pedersen, 1986; Panchenko & Vinogradov, 1985). Conversion between active and inactive forms depends on pH *in vitro* and is thought to depend on the state of mitochondrial energization *in vivo* (Van de Stadt *et al.*, 1973; Harris *et al.*, 1979; Husain & Harris, 1983), the inhibitor assuming its inactive form when mitochondria are energized and reverting to its active form upon collapse of the proton gradient. Milgrom (1991) has shown that F_1 inhibited by bmF_1I contains a single nucleotide trapped in a catalytic site. According to the binding change model, product release at one site is required for catalysis to occur at an alternate site (Kayalar *et al.*, 1977). Milgrom suggests that the inhibitor protein functions by blocking product release, thereby eliminating cooperative catalysis. It is possible that the physical basis for inhibition is steric hindrance of the conformational changes predicted to occur in alternating site catalysis and that this results in the trapping of one nucleotide in a catalytic site.

Despite a great deal of interest in bmF_1I and its physiological function, the exact mechanism by which the unidirectional inhibition occurs remains unclear. The amino acid sequences of the inhibitor proteins from beef heart, *S. Cerevisiae*, and *C. utilis* mitochondria have been determined (Walker *et al.*, 1987; Matsubara *et al.*, 1981; Dianoux & Hoppe, 1987) and display a high degree of homology, especially in the region corresponding to amino acid residues Arg35 to Lys46 of the bovine protein. This conserved region represents a possible target for further investigation by site-directed mutagenesis. In order to perform detailed structure/function studies on

† This work was supported by American Heart Association—Florida Grant 91GIA/709 to S.M.S. and G.V.H., U.S. Army Research Office Grant DAAL03-91-G-0061 to P.-S.S., and NIH Grant NS 22695 to G.S.

* Address correspondence to this author at the Department of Molecular Biology, K-681.4.46, CIBA, CH-4002 Basel, Switzerland. Phone: 41 61 696 83 39; Fax: 41 61 696 93 01.

‡ Protein Expression Laboratory, Interdisciplinary Center for Biotechnology, Research, University of Florida.

§ University of Nebraska—Lincoln.

∥ Department of Biochemistry and Molecular Biology, University of Florida.

⊥ Department of Neuroscience, University of Florida.

® Abstract published in *Advance ACS Abstracts*, September 1, 1993.

[1] Abbreviations: IPTG, isopropyl 1-thio-β-D-galactopyranoside; bmF_1I, bovine heart mitochondrial F_1-ATPase inhibitor protein; ompA, outer membrane protein A; CD, circular dichroism; θ, mean residue molar ellipticity; KPB, potassium phosphate buffer.

0006-2960/93/0432-10140$04.00/0

A

```
1                                                  31
ggt acc cgg GGA TCC GAA TCT GGT GAC AAC GTT CGG AGC TCT GCT GGT GCT GTT CGC GAC
 KpnI  SmaI  G   S   E   S   G   D   N   V   R   S   S   A   G   A   V   R   D

61                                                 91
GCA GGT GGT GCT TTC GGT AAA CGT GAA CAG GCT GAA CAG GAG CGC TAC TTC CGT GCT CGA
 A   G   G   A   F   G   K   R   E   Q   A   E   Q   E   R   Y   F   R   A   R

121                                               151
GCT AAA GAA CAG CTG GCT GCT TTA AAA AAA CAT CAT GAA AAC GAG ATA TCT CAT CAT GCC
 A   K   E   Q   L   A   A   L   K   K   H   H   E   N   E   I   S   H   H   A

181                                               211
AAG GAA ATC GAA CGT CTG CAG AAA GAA ATC GAA CGT CAT AAA CAA TCG ATA AAA AAG CTT
 K   E   I   E   R   L   Q   K   E   I   E   R   H   K   Q   S   I   K   K   L

241                                               270
AAA CAG TCT GAA GAC GAC GAC TAA gaa ttc
 K   Q   S   E   D   D   D  OCH  EcoRI
```

B

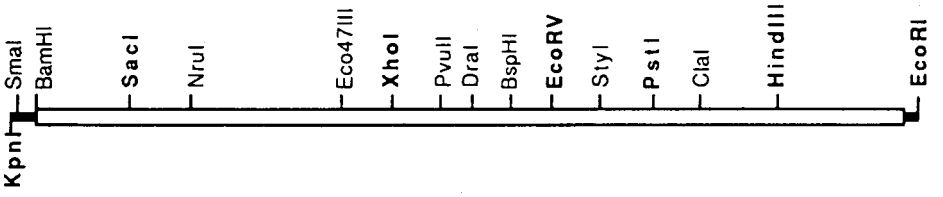

FIGURE 1: (A) Nucleotide sequence of the synthetic gene designed for the bmF$_1$ inhibitor protein. The coding sequence is shown in upper case, the linking sequence in lower case. The bracketing *Sma*I and *Eco*RI restriction enzyme sites are indicated and underlined, and the stop codon is shown in bold. Restriction enzyme sites present in the synthetic gene are underlined. The corresponding amino acid sequence is shown in one-letter code underneath the nucleotide squence. (B) Schematic presentation of the restriction enzyme site distribution in the bmF$_1$I synthetic gene. Sites shown in bold were used during assembly of the entire gene and bracket individual oligonucleotides. The dark bar on each end represents linking sequences containing cloning sites.

bmF$_1$I and investigate which amino acid residues in bmF$_1$I are important for binding to F$_1$ and inhibition of F$_1$-ATPase activity, a recombinant bmF$_1$I protein that can be easily obtained in large quantities would be extremely useful.

This paper reports the design, construction, and cloning in *E. coli* of a synthetic gene that codes for beef heart mitochondrial F$_1$I. This gene was fused to the coding sequence for the outer membrane protein A (ompA) signal sequence and placed under the control of a strong inducible *E. coli* promoter. Biologically active recombinant bmF$_1$I was recovered from the periplasmic space of *E. coli* and purified in a single step to near homogeneity. In addition, theoretical analyses of the primary structure were performed and supplemented by detail circular dichroism studies to probe the conformation of F$_1$I under different conditions of pH and temperature. Implications of these findings are discussed in terms of overall structure and function of the inhibitor protein.

EXPERIMENTAL PROCEDURES

Strains and Plasmids. *E. coli* K-12 strain XL1-Blue (*recA1, endA1, gyrA96, thi-1, hsdR17, supE44, RelA1, lac,* [*F' ProAB, lacI^{q}ZDM15, Tn10*(*tet^r*)]) (Stratagene), CAG-456 [*lac*am *trp*am *pho*am *supC^{ts} rpsL*(Sm^R) *mal* am *htpR*165] (Baker *et al.*, 1984), and BL21(DE3) (F$^-$ *ompT* r_B–$m_B$$^-$) were used for the routine cloning and expression experiments. Plasmid pAL5 was derived from pIN-III-ompA (Ghrayeb *et al.*, 1984), which was a kind gift from M. Inouye.

Materials. Restriction enzymes, calf intestinal phosphatase, and T4 DNA ligase were from New England Biolabs or promega. T4 polynucleotide kinase and a Sequenase II DNA sequencing kit were from US Biochemicals Corp. Immunoblotting reagents, KH_2PO_4, and K_2HPO_4 (ACS grade) were purchased from Sigma. Oligonucleotides were synthesized on an ABI Model 380B-02 (Applied Biosystems Inc.) DNA synthesizer. N-Terminal amino acid sequence analysis and DNA synthesis were performed by the Protein Chemistry Core and DNA Synthesis Core Facilities of the University of Florida Interdisciplinary Center for Biotechnology Research, respectively.

Construction of a Synthetic Gene for Bovine Heart Mitochondrial F$_1$I. The amino acid sequence of the bovine heart mitochondrial F$_1$-ATPase inhibitor protein (Fragione *et al.*, 1981) was back-translated into a DNA sequence using codons preferred by *E. coli* for abundantly expressed proteins (de Boer & Kastelein, 1986). This sequence was edited to contain 13 unique restriction enzyme sites distributed throughout the gene without altering the encoded amino acid sequence. Extra *Sma*I and *Eco*RI restrictin enzyme sites were designed at the 5′- and 3′-ends of the sequence, respectively. This allowed insertion of the F$_1$I coding sequence in the correct translational reading frame in the expression vector pAL5. The resulting DNA sequence, its restriction enzyme sites, and the oligonucleotides used to assemble the gene are shown in Figure 1.

Six sets of complementary oligonucleotides ranging in size from 26 to 90 bases were synthesized. Individual oligonucleotides were phosphorylated (Sambrook *et al.*, 1989) at a concentration of 1.5 pmol/μL, pooled with their complementary oligonucleotide, heated to 95 °C for 5 min, and cooled slowly to room temperature to anneal. Double-stranded oligonucleotides 5 and 6 were cloned pairwise in pTZ19R (Pharmacia) while oligonucleotides 3 and 4 were inserted

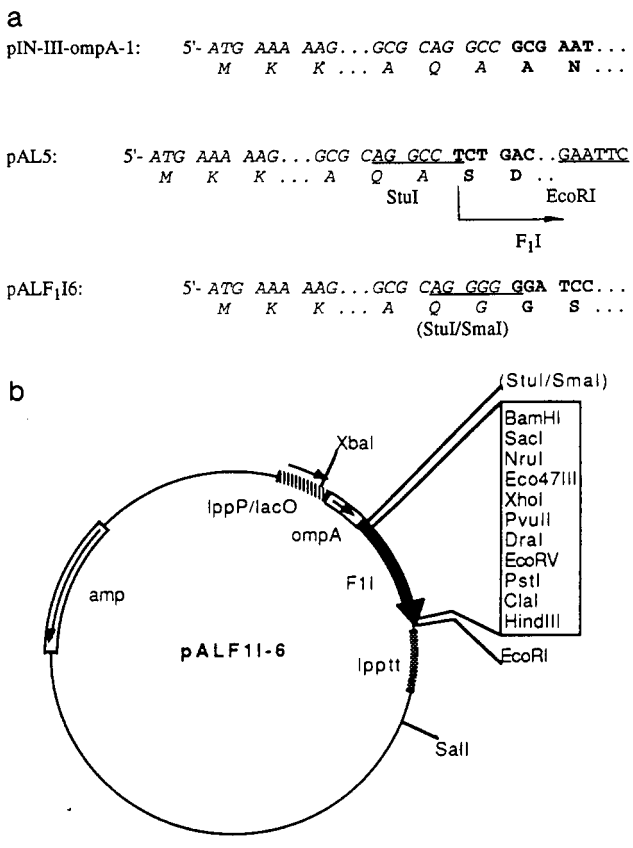

FIGURE 2: (A) Pertinent nucleotide (top line) and amino acid (bottom line, one-letter code) sequence around the ompA signal sequence cleavage site in pIN-III-ompA, pAL5, and pALF$_1$I6. The cleavage site is indicated by the arrow. The signal sequence is shown in italics. The underlined sequence for pAL5 indicates the *Stu*I restriction enzyme site, while the underlined sequence for pALF*1I6* represents the *Sma*I site of F$_1$I cloned into the *Stu*I site (both sites cancer each other out). (B) *E. coli* expression plasmid pALF$_1$I6. The hybrid lipoprotein promoter/lactose operator drives the transcription of the fusion ompA-F$_1$I gene. Restriction enzyme sites present in the F$_1$I coding sequence are boxed. Abbreviations used are as follows: lppP, lipoprotein promoter; lpptt, lipoprotein gene transcription termination signal; lacO, lactose operator; amp, ampicillin resistance gene.

pairwise in pBlueScript$^-$(KS) (Stratagene). Oligonucleotides 1 and 2 were cloned separately in pBlueScript$^-$(KS). Individual clones for each set of oligonucleotides were sequenced using the dideoxy method (Sambrook *et al.*, 1989), and mutation-free clones were combined by standard cloning procedures to assemble the intact F$_1$I coding sequence. The resulting construct contained the complete F$_1$I synthetic gene in a hybrid pTZ19R/pBlueScript$^-$(KS) plasmid named pBS.TZ.F$_1$I.

Construction of the Expression Plasmid pALF$_1$I6. Plasmid pAL5 was derived from pIN-III-ompA (Ghrayeb *et al.*, 1984) by construction of a unique *Stu*I restriction enzyme site encompassing the C-terminal alanine codon of the ompA signal sequence (Van Heeke, unpublished results; see Figure 2A). pBS.TZ.F$_1$I was digested with the restriction enzymes *Sma*I and *Eco*RI, while pAL5 was digested with *Stu*I and *Eco*RI. The reaction mixtures were separated on a 1% low gelling temperature agarose gel (SeaPlaque, EMC), and the 257 base pair F$_1$I fragment was ligated to the pAL5 vector using an in-gel ligation method (Sheng *et al.*, 1992). *E. coli* K-12 strains XL1-Blue was transformed with an aliquot of this ligation mixture using the procedure described by Hanahan (1983). Single colonies were grown in L broth supplemented with ampicillin at 37 °C for 18 h, and plasmid DNA was isolated and analyzed by restriction enzyme mapping following standard procedures (Sambrook *et al.*, 1989). One of the positive clones, pALF$_1$I6 (shown in Figure 3), was used for further expression experiments. *E. coli* K-12 CAG-456 and BL21(DE3) were also transformed with pALF$_1$I6.

Expression of Recombinant Bovine Heart Mitochondrial F$_1$I in E. coli. E. coli K-12 strains XL1-Blue and CAG-456 containing pALF$_1$I6 were cultured at 37 °C in 5 mL of L broth supplemented with 50 μg/mL ampicillin for 18 h. The culture was diluted 100-fold in fresh growth medium and incubated until the optical density measured at 550 nm reached 0.8–1.0. IPTG was added to a final concentration of 2 mM, and incubation was continued at 37 °C for 3 h. Cells were harvested, washed, and resuspended in ice-cold 50 mM Tris (pH 7.6)/1 mM EDTA at a final concentration of 20 mL·OD/mL (equivalent to 20 mL of a culture at an optical density of 1 per milliliter of wash solution). Phenylmethanesulfonyl fluoride was added to a 1 mM final concentration, and the cell suspension was sonicated three times for 30 s on ice. Cell extracts were centrifuged at 16000*g* for 10 min. The pellet and supernatant fractions were dissolved in equal volumes of protein sample buffer (containing 2% sodium dodecyl sulfate and 20% β-mercaptoethanol) and fractionated on a denaturing 12% Tris–Tricine polyacrylamide gel (Schagger & von Jagow, 1987). Total cell proteins were visualized by Coomassie Brilliant Blue staining. For detection of recombinant F$_1$I, polyacrylamide gel-fractioned cell extracts were transferred to an Immobilon-P membrane using a Bio-Rad electroblotter and probed with rabbit polyclonal antibodies raised earlier against a recombinant F$_1$I fusion protein (Van Heeke *et al.*, 1993). Immunoreactive protein bands were visualized using an alkaline phosphatase-conjugated anti-IgG secondary antibody and a color development reaction mixture containing Nitro Blue Tetrazolium and 5-bromo-4-chloro-3-indolyl phosphate.

One-Liter Scale Production and Purification of Recombination bmF$_1$I from E. coli. A 1-L culture of *E. coli* CAG-456 or BL21(DE3) containing pALF$_1$I6 was grown and induced as described above for the 5-mL culture. After a 3-h incubation at 37 °C, cells were harvested and washed as described above. The cell pellet was then resuspended in 100 mL of an ice-cold solution of 1 M Tris (pH 9.0)/2 mM EDTA and kept on ice for 30 min. The cell suspension was centrifuged for 10 min at 16000*g* at 4 °C, and the supernatant fraction, containing most of the recombinant bmF$_1$I, was saved.

One-sixth of the recovered supernatant fraction was dialyzed at 4 °C against 0.02 M Na_2HPO_4/citric acid (pH 6.7) containing 0.5 mM EDTA and 0.5 mM EGTA and applied to a CM-Cellex (Bio-Rad) cation-exchange resin at 4 °C. The column was washed with 1 bed volume of the same buffer, and recombinant bmF$_1$I was eluted with 2 bed volumes of a linear gradient of 0.02 M Na_2HPO_4/citric acid (pH 6.7) to 0.1 M Na_2HPO_4/citric acid (pH 8.7) containing 0.5 mM EDTA and 0.5 mM EGTA, followed by 2 bed volumes of 0.1 M Na_2HPO_4/citric acid (pH 8.7)/0.5 mM EDTA and 0.5 mM EGTA. Thirty-one fractions of 5 mL each were collected, and a trichloroacetic acid-precipitated aliquot of each was analyzed on a denaturing 12% Tris–Tricine polyacrylamide gel. Those fractions containing highly enriched F$_1$I were pooled and concentrated on a Centriprep-10 filter (Amicon).

Preparation and Assay of F$_1$I-ATPase. F$_1$-ATPase depleted of F$_1$I was purified from beef heart mitochondrial paste by the method of Knowles and Penefsky (1972a,b) as modified by Gruys *et al.* (1985). The specific activity of the beef heart F$_1$ used in these experiments was 42 and 32 units/(min·mg of F$_1$) at pH 6.7. *S. cerevisiae* F$_1$-ATPase was prepared by

chloroform extraction of submitochondrial particles and was not further purified. ATP hydrolysis was measured at 30 °C by a coupled assay described (Ebel & Lardy, 1975). Reactions contained 1 μg/mL beef heart F$_1$-ATPase, 20 mM Tricine, 20 mM PIPES, 2 mM $MgCl_2$, 0.45 mM NADH, 2 mM phosphoenolpyruvate, 6.5 mM KCl, and 4 units/mL of both lactic dehydrogenase and pyruvate kinase. The pH of the assay mixture was adjusted to either 6.7 or 8.0. The 100-fold excess of coupling enzymes relative to the F$_1$-ATPase ensures that the coupling enzymes are not rate-limiting at any pH or substrate concentration used. This was confirmed by measuring reaction velocities at fixed substrate concentrations and varied enzyme concentrations. The concentration of Mg-ATP was 0.3 mM for assays at pH 8.0 and 0.4 mM for assays at pH 6.7. Under these conditions the linear range of the reaction extended for at least 10 min. Inhibition by bmF$_1$I was assayed by addition of various amounts of bmF$_1$I to the reaction mixture. Reactions were started by addition of enzyme and were incubated for 10 min. Rates were calculated from 6 to 9 min to ensure that the inhibitor protein had assumed its active state. Substrate concentrations were 0.4 mM at pH 6.7 and 0.3 mM at pH 8.0 for inhibition of F$_1$-ATPase by total periplasmic fractions.

The concentration of purified bmF$_1$I was determined by quantitative amino acid analysis performed at the Protein Chemistry Core Facility of the University of Florida Interdisciplinary Center for Biotechnology Research.

Circular Dichroism Experiments. CD experiments were performed on a Jasco J600 spectropolarimeter equipped with a water-jacketed cuvette of 1-mm path length (Hellma, Mullheim, Germany) for F$_1$I concentrations of 5–20 μM F$_1$I, or a 10-mm cuvette for F$_1$I concentrations lower than 5 μM. A PolyScience Circulator water bath, Model 9100 (flow rate 600 mL/min), was used to adjust the temperature of the CD cell. The parameters used for the measurements were as follows: sensitivity, 50 mdeg; time constant, 1 s; scan speed, 20 nm/min; wavelength resolution, 0.1 nm; 3–5 scans per spectrum. The spectropolarimeter was calibrated with bovine serum albumin and a 0.06% (w/v) aqueous ammonium *d*-10-camphorsulfonate solution as described by the manufacturer. The protein sample was diluted from a stock solution to the desired concentration in 20 mM KPB/pH 6.7 or 8.0 or 100 mM KPB/pH 4.0 or 8.0 (mixture of mono- and dibasic potassium phosphate) and incubated in the CD cell at the desired temperature for 20–30 min prior to analysis. The lower F$_1$I concentrations were verified and corrected using $\theta_{204} = -13\,656$ deg cm^2 dmol^{-1} (determined with the 10 μM sample), which corresponds with the isoelliptic point for F$_1$I, as a standard.

Melting curves were recorded at a fixed wavelength of 222 nm. The temperature in the CD cell was measured with a temperature probe. The sample was equilibrated at each temperature for 2 min prior to data recording. F = the ratio of the θ_{222} at a particular temperature to the θ_{222} at 0.3 °C for concentrations below 5 μM and relative to θ_{222} at 2 °C for concentrations above 5 μM. The melting curves in Figure 7 and 8 represent unsmoothed data. The melting temperature was determined as the minimum of the first derivative of the mathematically smoothed melting curve.

RESULTS AND DISCUSSION

Design and Construction of a Synthetic Gene for bmF$_1$I. The amino acid sequence as published by Frangione *et al.* (1981) was used to design a DNA sequence coding for bmF$_1$I. This sequence differs in one residue (position 30) from the sequence as deduced by Walker *et al.* (1987). Condons preferred by *E. coli* for highly expressed genes were used in the design of the coding sequence. This sequence was then edited to contain 13 unique restriction enzyme sites without altering the encoded amino acid sequence. The final coding sequence was synthesized as six sets of complementary oligonucleotides which were cloned individually or pairwise in pTZ19R or pBlueScript$^-$(KS) (see Experimental Procedures). The nucleotide sequence of the individual oligonucleotide clones was verified prior to assembling the complete gene. The final bmF$_1$I coding sequence in pBS.TZ.F$_1$I was flanked by a *Sma*I restriction enzyme site at the 5′-end and an *Eco*RI restriction enzyme site at the 3′-end (see Figure 1B).

Construction of the Expression Plasmid. Upon digestion of pBS.TZ.F$_1$I with *Sma*I and *Eco*RI, the 257 base pair F$_1$I encoding fragment was recovered and subcloned in the bacterial expression plasmid pAL5. pAL5 is a derivative of pIN-III-ompA. The resulting plasmid, pALF$_1$I6, was used for expression studies. In this construct, transcription of the F$_1$I coding sequence is driven by the strong lipoprotein promoter and regulated by the lactose operator. The resulting mRNA translates into a fusion protein of the 21 amino acid outer membrane protein A (ompA) signal sequence and recombinant bmF$_1$I. While the ompA signal sequence will direct any attached protein to the periplasmic space, successful translocation across the membrane will depend on the secretion compatibility of the fused protein. Since the mitochondrial F$_1$I is encoded in the nucleus, it is capable of traversing membranes. Targeting proteins to the periplasm of *E. coli* has many advantages, including a higher probability for correct folding and less susceptibility to proteolytic degradation. In addition, subsequent purification is facilitated since considerably fewer proteins are present in the periplasm compared to the cytoplasm.

Insertion of the F$_1$I sequence in the pAL5 vector caused the alanine residue at position 21 of the ompA-F$_1$I fusion protein to be replaced by a glycine residue. This alanine residue is part of the AQA triplet which represents the −3, −1 rule for signal sequences (Von Heijne, 1983) and has been shown to be important for correct signal sequence processing by *E. coli* signal peptidase I. Substitution of this alanine residue by another small side-chain amino acid residue should have little effect on the correct processing of the signal sequence, although it may influence the rate of cleavage.

Expression of Recombinant bmF$_1$I. *E. coli* XL1-Blue, CAG-456, and BL21(DE3) were transformed with pALF$_1$-I6, and expression and localization of recombinant bmF$_1$I were monitored. As can be seen in Figure 3, production of bmF$_1$I was plasmid- and IPTG-dependent. Western analysis with polyclonal antibodies raised against F$_1$I shows an immunoreactive band in cell extracts from *E. coli* XL1-Blue and CAG-456 containing the expression plasmid pALK$_1$I6, but not in cell extracts from *E. coli* lacking the plasmid. Furthermore, the production of bmF$_1$I was clearly induced by IPTG. A basal level of leaky expression was found in noninduced cell cultures when grown in L broth. Some of the recombinant bmF$_1$I protein was found in the pellet fraction. However, part of this pellet fraction represents nonlysed cells. In addition, some ompA-F$_1$I precursor which did not quite resolve from the correctly processed form may also be present in this fraction. A weak immunoreactive band with an estimated molecular mass of 38 kDa is also found in lanes 1 and 2, while a smaller and even weaker immunoreactive band

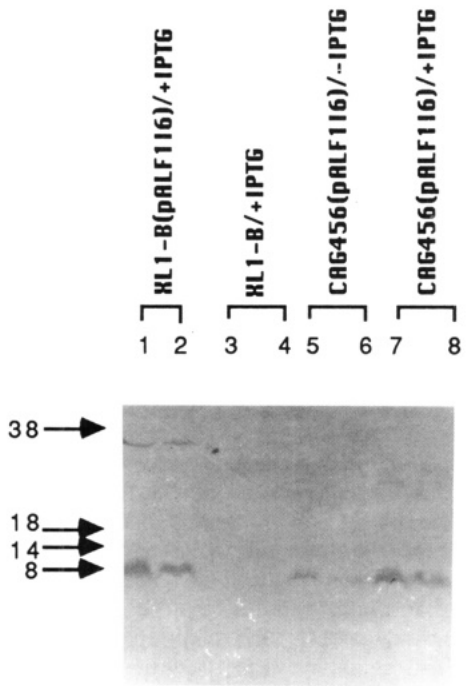

FIGURE 3: Immunoblot of fractionated total *E. coli* cell extracts. Cell extract was fractionated on a denaturing 12% Tris–Tricine polyacrylamide gel and transferred to an Immobilon-P membrane. Immunoreactive bands were detected as described in the Experimental Procedures. Lanes 1 and 2: Total cell extract from *E. coli* XL1-Blue containing pALF$_1$I6 grown under inducing conditions. Lanes 3 and 4: Total cell extract from *E. coli* XL1-Blue not containing any plasmid and grown under inducing conditions. Lanes 5 and 6: total cell extract from *E. coli* CAG-456 containing pALF$_1$I6 grown under noninducing conditions. Lanes 7 and 8: Total cell extract from *E. coli* CAG-456 containing pALF$_1$I6 and grown under inducing conditions. Odd-numbered lanes: soluble fraction of cell extract; even-numbered lanes: pellet fraction after cell lysis.

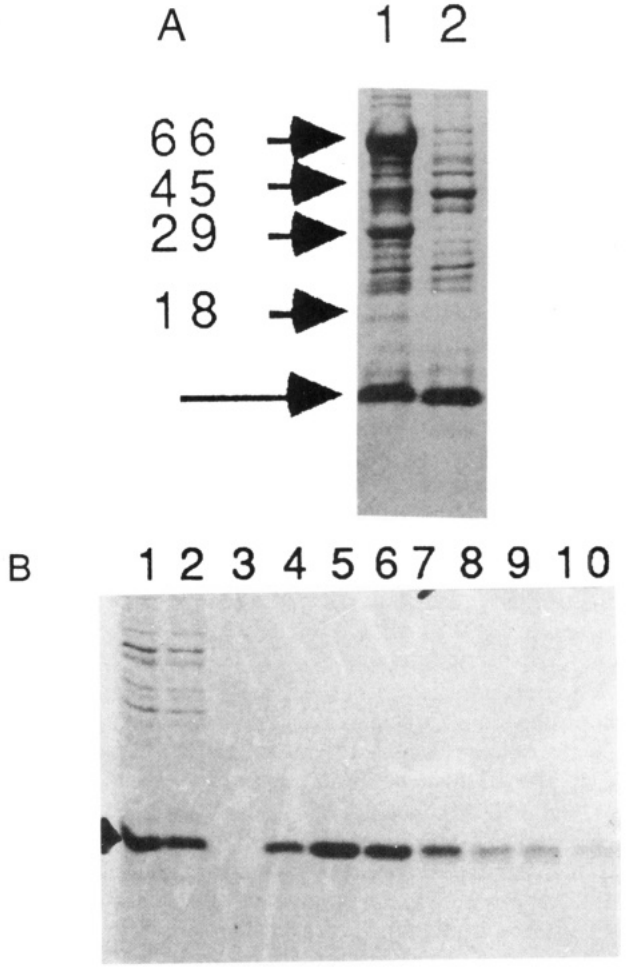

FIGURE 4: (A) Coomassie Blue-stained denaturing polyacrylamide gel. Total proteins released by osmotic shock from induced cultures of *E. coli* CAG-456 (lane 1) and BL21(DE3) (lane 2) containing pALF$_1$I6. Equal extracts from normalized cell pellets were loaded in each lane. The position of molecular weight markers is shown by arrows on the left. The large arrow at the bottom on the left indicates the position of bmF$_1$I. (B) Single-step purification of recombinant bmF$_1$I from a 1-L culture of *E. coli* BL21(DE3) containing pALF$_1$-I6. Samples were loaded on a denaturing polyacrylamide gel (see Experimental Procedures), and proteins were visualized by Coomassie Blue staining. Lane 1: Dialyzed periplasmic fraction before loading on the CM-Cellex column. Lane 2: Flow-through of the CM-Cellex column. Lanes 3–10: Fractions of the elution gradient containing recombinant bmF$_1$I.

is found in lanes 5 and 7. These probably represent some nonspecific cross-reaction of the polyclonal antiserum.

E. coli K-12 CAG-456 has a mutant *htpR* locus. A marked increase in heterologous protein production had been observed in some cases when using this *E. coli* strain (Rimm & Pollard, 1989), presumably because this mutation causes a nonspecific defect of proteolytic enzymes. However, production of recombinant bmF$_1$I was not noticeably higher in this host than in *E. coli* XL1-Blue (see Figure 3).

E. coli strain BL21(DE3) (Studier *et al.*, 1990) lacks both the outer membrane protease T (ompT) and the *lon* protease (Goff & Goldberg, 1985) and was also tested for increased F$_1$I production. Although the amount of bmF$_1$I produced in BL21(DE3) was not significantly higher than in the other *E. coli* hosts tested, the abundance of bmF$_1$I relative to the other periplasmic proteins was greater (see below). For this reason and others detailed below, *E. coli* strain BL21(DE3) was the preferred host for the production of recombinant bmF$_1$I.

Next, localization of the recombinant F$_1$I was determined. Cells harvested from induced cultures were subjected to an osmotic shock procedure, and the recovery of bmF$_1$I was monitored. Most of the recombinant bmF$_1$I was released to the supernatant fraction after treatment of the cells for 20 min with a solution of 1 M Tris/2 mM EDTA (pH 9.0) (see Figure 4A). Some bmF$_1$I remained in the cell pellet which could be recovered by an additional wash with cold distilled water (data not shown). However, many other proteins also cofractionated during this treatment. The single-step 1 M Tris osmotic shock resulted in a high enrichment of bmF$_1$I and served as a good starting point for subsequent purification. A small portion of the bmF$_1$I fraction that was left in the cell pellet migrated at a slower rate on a denaturing protein gel (data not shown). This portion probably represents some unprocessed precursor still containing the signal sequence. It was not determined whether this was due to the replacement of alanine by glycine at the ompA signal sequence cleavage site. The bmF$_1$I protein recovered from the osmotic shock procedure was detected as a single bond on a denaturing protein gel by immunoblotting with polyclonal antiserum (data not shown).

Fractions obtained after osmotic shock from *E. coli* CAG-456 and BL21(DE3) containing bmF$_1$I were analyzed on a denaturing polyacrylamide gel (see Figure 4A). While similar amounts of bmF$_1$I were recovered, considerably less total protein was present in the *E. coli* BL21(DE3) periplasmic fraction. In particular, two prominent proteins with estimated molecular masses of 29 and 60 kDa present in the *E. coli* CAG-456 periplasmic fraction were not found in *E. coli* BL21-(DE3).

The total protein mixture obtained after the osmotic shock procedure was electrotransferred to an Immobilon-P membrane, and the Coomassie Brilliant Blue-stained protein band representing bmF_1I was subjected to N-terminal amino acid sequence analysis. The amino acid sequence of this protein matched that of native bmF_1I for at least the first 10 residues. This further confirms the identity of the recombinant protein and indicates a correct and complete processing of the ompA signal sequence for that portion of bmF_1I that was released from the periplasm by osmotic shock. This also indicates that substitution of glycine for alanine as the C-terminal residue of the ompA signal sequence does not affect correct cleavage of the signal sequence.

Purification of Recombinant bmF_1I from E. coli. One-liter cultures of *E. coli* BL21(DE3) containing $pALF_1I6$ were grown. At the time of induction, IPTG was added to a 2 mM final concentration. The periplasmic fraction containing recombinant bmF_1I was recovered by osmotic shock and processed as described in the Experimental Procedures. As can be seen from Figure 4B, this single cation-exchange chromatography step resulted in nearly pure recombinant bmF_1I. Lane 1 shows the total periplasmic fraction proteins of *E. coli* BL21(DE3) containing $pALF_1I6$ as recovered by osmotic shock and upon dialysis against the cation-exchange loading buffer. Lane 2 of Figure 4B shows that the flow-through of that resin still contains a small amount of bmF_1I which was recoverable by a second chromatography step over a regenerated CM-Cellex column, suggesting that the column had been overloaded. The following lanes in Figure 4B represent fractions collected from the gradient elution, showing nearly pure bmF_1I. The recombinant inhibitor protein started eluting at 80 mM Na_2HPO_4/citric acid, pH 8.07, containing 0.5 mM EDTA and 0.5 mM EGTA.

Purification of bmF_1I from *E. coli* CAG-456 following the same protocol always resulted in the copurification of a 60-kDa protein. Neither different conditions during cation-exchange chromatography nor any extra anion-exchange chromatographic or gel filtration steps could resolve the bmF_1I from this protein. However, this 60-kDa protein, as well as another 29-kDa protein was clearly less abundant in the periplasmic extract from *E. coli* BL21(DE3) (see Figure 4A), making this host superior for the overproduction and recovery of bmF_1I. Purification of recombinant bmF_1I from an overproducing *E. coli* BL21(DE3) host represents a vast improvement over previous procedures using bovine heart mitochondria. This rapid and simple purification scheme was possible only because of the high amounts of recombinant bmF_1I expressed in *E. coli* BL21(DE3) and its targeted location, where it is highly abundant relative to the periplasmic proteins. Two milligrams of recombinant bmF_1I has been purified by this single-step procedure from a 160-mL culture of *E. coli* BL2(DE3) containing $pALF_1I6$, corresponding to 12 mg of pure F_1I protein from a 1-L culture.

Sensitivity of Beef Heart F_1-ATPase to Purified Recombinant bmF_1I. Recombinant bmF_1I was isolated and assayed (Figure 5) as described in the Experimental Procedures. The inhibitor protein was added to the reaction mixture from an aqueous stock solution at pH 8.0. Inhibition of beef heart F_1-ATPase by purified recombinant bmF_1I was pH-sensitive, saturable, and turnover-dependent. A bmF_1I concentration of 1.0 μM inhibited the rate of ATP hydrolysis at pH 6.7 by about 80%. The inhibition at pH 8.0 for the same inhibitor concentration was about 22%. Maximal inhibition at pH 6.7 was obtained at a concentration of about 1.0 μM, and half-maximal inhibition occurs at about 0.4 μM. Interestingly,

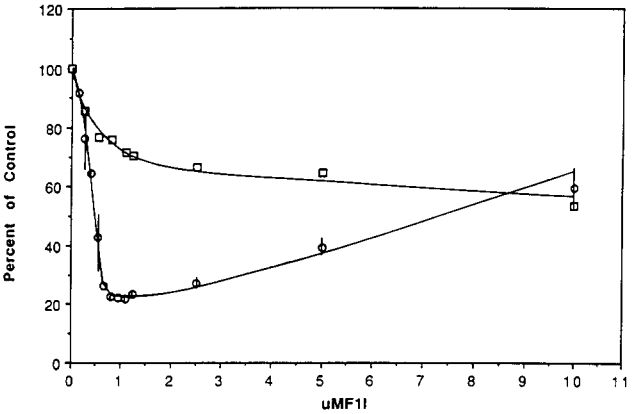

FIGURE 5: Inhibition of beef heart F_1-ATP by purified recombinant bmF_1I. F_1-ATPase activity was assayed at pH 6.7 (circles) and pH 8.0 (squares) as described under Experimental Procedures. Rates are expressed as a percentage of the rates measured in the absence of bmF_1I. Values determined at pH 6.7 are the average of 2–5 measurements. The error bars show the actual range of the data. Values determined at pH 8.0 are single measurements.

Table I: Turnover Dependence of Recombinant bmF_1I[a]

	rates [μmol/(min·mg)]	
[bmF_1I] (μM)	0–1 min	6–9 min
0.00	25.6	22.7
0.16	22.8	17.7
0.40	23.1	15.5
0.80	19.9	8.7
1.60	22.9	6.6

[a] Beef heart F_1-ATPase activity was measured at pH 6.7 in the presence of various concentrations of purified bmF_1I as described in the Experimental Procedures. The inhibitor protein was added from a 41 μM stock solution at pH 8.0. The data represent a single experiment which was reproduced twice. Absorbance at 340 nm was recorded every 13 s during the experiment.

higher concentrations resulted in less inhibition of ATP hydrolysis at pH 6.7 (Figure 5). At a concentration of 10 μM, F_1I inhibited about 3-fold less than at 1.0 μM at pH 6.7. ATPase activity was also measured at five different fixed concentrations of bmF_1I with varied substrate concentration at pH 6.7. Dixon plots of these data gave a K_i of 0.2 μM and were typical of noncompetitive inhibition (data not shown). In each experiment the rate of ATP hydrolysis in the presence of bmF_1I declined after 1–2 min of assay (Table I). This result is consistent with the documented turnover dependence of bmF_1I (Cintron *et al.*, 1982) and with reports of the existence of an inactive, basic form of F_1I (Panchenko & Vinogradov, 1985). Recombinant bmF_1I also inhibited *S. cerevisiae* F_1-ATPase to a similar extent at pH 6.7 and 8.0 (data not shown).

Inhibition of F_1-dependent ATP hydrolysis by recombinant bmF_1I obtained from an overproducing *E. coli* culture by osmotic shock and used without further purification was also assayed. Similar results were obtained for this crude bmF_1I preparation compared to the purified inhibitor protein (data not shown). Periplasmic fractions from *E. coli* which did not express bmF_1I had no significant effect on ATP hydrolysis by either beef heart or *S. cerevisiae* F_1-ATPase. The fact that biological activity of recombinant bmF^1I can be determined in crude preparations of periplasmic fractions will be useful for the rapid screening of large numbers of mutant F_1I proteins without prior purification. This is in contrast to a just recently published report (Lebowitz & Pedersen, 1993), where the rat liver F_1I is expressed as an inactive fusion protein. These authors obtain about 1 mg of F_1I after a series of steps including a proteolytic cleavage.

Prediction of Structural Elements. The amino acid sequence of bovine mitochondrial F_1I was carefully examined to look for indications of likely three-dimensional structure. Computer programs which use Chou and Fasman and other algorithms all suggest that F_1I is primarily α-helical. Closer examination of the C-terminal region reveals a high charge density mixed with an isoleucine amino acid recurring four times every seven residues starting at position 53. Within this heptad repeat a leucine or histidine amino acid alternates at position 4 relative to the isoleucine residue. A similar sequence pattern is often found in regions of proteins known to contain a coiled-coil domain. These findings prompted us to analyze the primary structure of F_1I in more detail by a computer program designed to detect coiled-coil regions. This program was written and based on that described by Lupas *et al.* (1991) and compares the F_1I amino acid sequence with those found in typical coiled-coil containing proteins. It assigns a score to each amino acid in a sequence in all seven possible heptad frames. These scores are calculated from the frequency at which each amino acid is found in each of those positions (1–7) in known coiled-coil proteins. The geometric mean of these scores is then taken over a window of 28 amino acids. The window is chosen to be 28 amino acids long as this is likely the minimum sequence length required for coiled-coil formation. A geometrical mean score of 1.3 or above is claimed to indicate a probability greater than 50% that this sequence forms a coiled-coil *in vivo*, and scores of 1.5 and above indicate coiled-coils with virtual certainty (Lupas *et al.*, 1991). The F_1I sequences scored better than 1.3 over the entire region from residue 36 to the C-terminal residue number 84. Out of the 21 windows corresponding to this region 16 scored better than 1.5 and 2 scored 1.7 or better. These figures are comparable or in some cases better than those obtained for protein sequences known from structural data to define α-helical coiled-coils. Myosin and keratin score 1.70 and 1.44, respectively, for the amino acid region known to form a coiled-coil, while globular proteins and randomly generated sequences show a mean score of 0.8 and 0.78, respectively (Lupas *et al.*, 1991). It is therefore likely that the C-terminal 60% of F_1I defines a typical coiled-coil. As expected from their overall sequence homology, the C-terminal regions of the *S. cerevisiae* and *C. utilis* F_1I proteins also displayed a high score for coiled-coil probability when analyzed by this program.

In order to test this prediction, a series of CD experiments was performed at different temperatures. Since biological activity of F_1I is pH-dependent, its structure was also probed by CD analyses at different pH values.

Circular Dichroism Analysis of Purified Recombinant bmF$_1$I. Circular dichroism experiments were performed as described in the Experimental Procedures. In Figure 6, panels A and B show the mean residue molar ellipticity (θ) of 10 and 0.8 μM F_1I solutions, respectively, at different temperatures. Figure 6B shows the spectra down to only 197 nm, at which point the absorbance by the buffer became limiting in the 10-mm path length CD cell. The minimum and maximum peak positions recorded at 50 °C or lower indicate that F_1I is predominantly α-helical under these conditions. The spectra recorded at various temperatures displayed an isoelliptic point at 204 nm. This is the wavelength at which the 100% α-helical protein conformation and the random coil conformation exhibit the same θ and indicates that F_1I is principally α-helical and random coil with an increasing random coil conformation at the expense of α-helix as F_1I is heated.

The mean residue molar ellipticity measured at 222 nm (θ_{222}) was determined to be −31 470 deg cm^2 dmol^{-1} in 20 mM

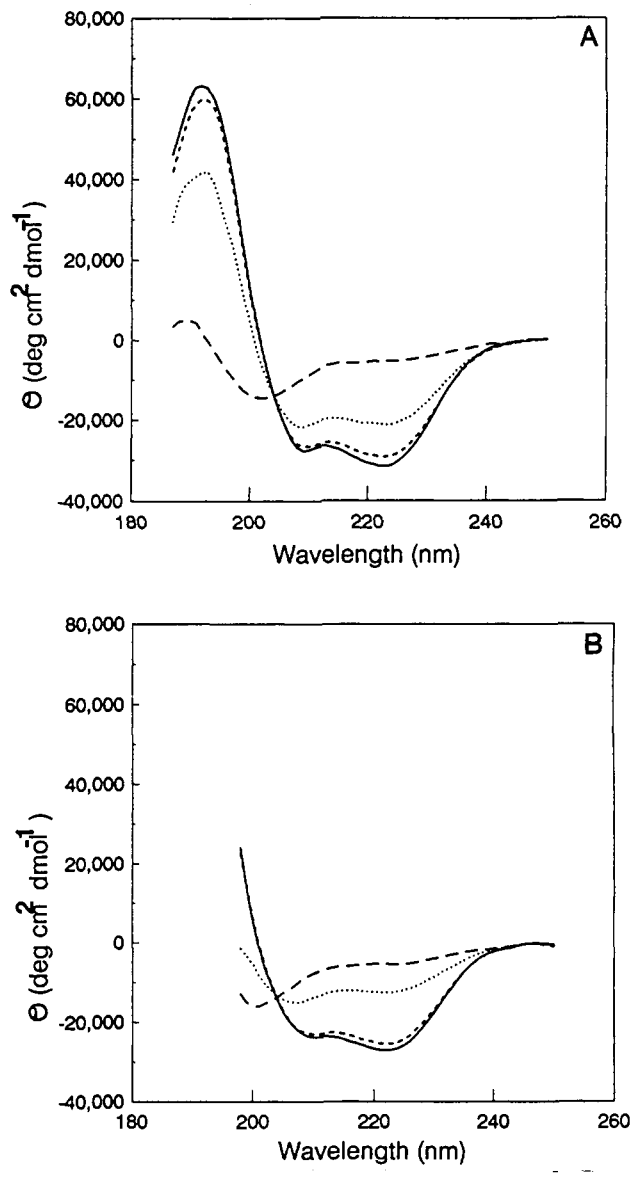

FIGURE 6: CD spectra of recombinant bmF_1I. (A) Spectrum for a 10 μM solution of F_1I in 20 mM KPB (pH 6.7) were recorded at 2 °C (—), 23 °C (- - -), 50 °C (···), and 75 C (– –). The θ_{222} value for F_1I at 2 °C was determined to be −31 470 deg cm^2 dmol^{-1}. (B) Spectrum for a 0.8 μM solution of F_1I in 20 mM KPB (pH 6.7) recorded at 0.3 °C (—), 20 °C (- - -), 49 °C (···), and 74 °C (– –). The θ_{222} value for F_1I at 0.3 °C was determined to be −26 880 deg cm^2 dmol^{-1}.

KPB (pH 6.7) at 2 °C for F_1I at a final concentration of 10 μM. Data points between 184 and 240 nm at 1-nm intervals were used to calculate the secondary structure content of F_1I at 2 °C in 20 mM KPB (pH 6.7) by the variable selection method (Manavalan & Johnson, 1987). This revealed a structural content of 85 ± 1% α-helix, 1 ± 1% parallel β-sheet, 11 ± 1% β-turn, and 5 ± 1% random coil, adding up to a total of 102% (root mean square error ≤ 0.552). A better fit was obtained using the data points between 187 and 240 nm. The secondary structure content was then calculated to be 84 ± 1% α-helical, 1 ± 1% parallel β-sheet, 1 ± 1% antiparallel β-sheet, 8 ± 1% β-turn, and 7 ± 1% random coil, adding up to a total of 101% (root mean square error ≤ 0.360). However, use of the variable selection method (Manavalan & Johnson, 1987) is only recommended when data points down to 184 nm or lower are included. Comparison of Figure 6A with Figure 6B shows a significantly lower α-helical content for F_1I at 0.8 μM versus 10 μM. The θ_{222} values for F_1I at a concentration

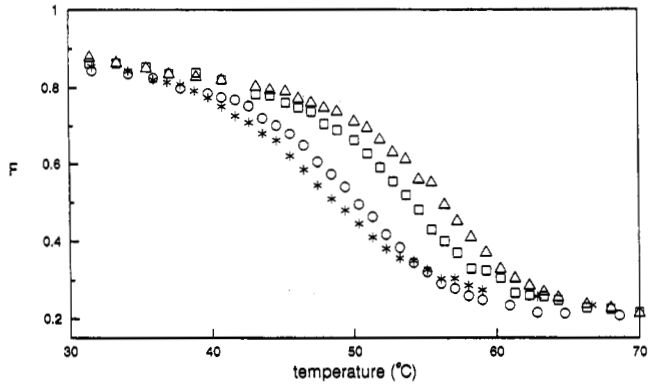

FIGURE 7: Thermal unfolding studies at pH 6.7 were performed on various concentrations of bmF$_1$I in 20 mM KPB as described in the Experimental Procedures. Since the θ_{222} value itself increases with increasing F$_1$I concentration, the *F* value (the ratio of the θ_{222} value at a particular temperature to the θ_{222} value at 0.3 °C for F$_1$I concentrations below 5 μM and to the θ_{222} value at 2 °C for concentrations above 5 μM) was plotted as a function of temperature. The melting temperature (T_m) for each concentration was determined from the first derivative of the methematically smoothed curve of this plot (not shown) and found to be 47.0, 51.8, 53.2, and 58.0 °C for F$_1$I at a concentration of 0.8 (stars), 1.5 (circles), 5 (squares), and 10 μM (triangles), respectively.

of 0.8 and 1.5 μM in 20 μM KPB (pH 6.7) at 0.3 °C were −26 880 and −28 180 deg cm^2 dmo^{-1}, respectively. This concentration-dependent change in α-helical content in F$_1$I at low temperatures is especially interesting in relation to the concentration-dependent inactivation of F$_1$I (see Figure 5). These data suggest that some specific interaction, accompanied by an increase in α-helical conformation, yields an inactive F$_1$I at higher concentrations.

The θ_{222} value obtained for F$_1$I in this study is different from the one published earlier. Frangione *et al.* (1981) reported a θ_{222} of −21 900 deg cm$_2$ dmol^{-1} for F$_1$I in 10 mM KPB at pH 6.9. They calculated a 50% α-helical content for F$_1$I. However, no information on the wavelength range, temperature, or instrument, nor the method used to predict the secondary structure, was given. On the basis of their θ_{222} value and using the method of Chen *et al.* (1974), we calculated a 64.6% α-helical content.

More detailed structural information could be obtained by analyzing the CD signal as a function of temperature. Therefore, a number of thermal unfolding studies were performed on recombinant bmF$_1$I. The protein was equilibrated at different concentrations in 20 mM KPB in the CD cell at the lowest possible temperature (0.3 °C for the 10-mm cell and 2 °C for the 1-mm cell) for 20–30 min. The ellipticity was measured at 222 nm as a function of temperature as described in the Experimental Procedures. Figure 7 shows the melting behavior of F$_1$I at various concentrations in 20 mM KPB (pH 6.7). The melting curves were mathematically smoothed, and the minimum of their first derivative (not shown) defined the melting temperature (T_m) for F$_1$I at a particular protein concentration. From Figure 7 can be seen that the T_m is concentration-dependent, higher concentrations resulting in higher T_m values. The T_m values measured were 47.0, 51.8, 53.2, and 58.0 °C for F$_1$I at concentrations of 0.8, 1.5, 5, and 10 μM, respectively, in 20 mM KPB at pH 6.7 (see Figure 7). For F$_1$I at a concentration of 20 μM in 20 mM KPB (pH 6.7) the T_m was 59 °C (data not shown). This concentration dependence is indicative of stabilizing interactions between F$_1$I molecules. The thermal stability is also remarkably high for an α-helical protein and is comparable to the thermal stability found in coiled-coil proteins. For instance, O'Shea *et al.* (1989) reported a T_m for a 33 amino acid peptide corresponding to the leucine zipper region of the yeast transcription factor GCN4 of 57 °C at a concentration of 34 μM.

Reversibility of the melting behavior was analyzed for F$_1$I at a 20 μM concentration, and the melting and reverse melting curves were found to be virtually superimposable (data not shown). This suggests that the thermal unfolding of F$_1$I is reversible. When purified recombinant F$_1$I was heated to 75 °C and cooled quickly to 23 °C, the obtained spectrum was virtually identical to the one obtained before heating (data not shown). This again suggests a complete recovery of the α-helical conformation. The heat stability of the inhibitory activity of this protein has been reported earlier (Frangione *et al.*, 1981) and has been exloited in some purification schemes (Ebner & Maier, 1977; Horstman & Racker, 1973). The data presented here are consistent with those earlier findings.

The inhibitory activity of F$_1$I is strongly pH-dependent. Therefore, the effect of pH on gross overall structure of F$_1$I was also investigated. The CD spectra recorded in 20 mM KPB (pH 8.0) at 0.3 °C revealed a θ_{222} value of −29 450 and −26 840 deg cm^2 dmol^{-1} for F$_1$I at concentrations of 1.8 and 0.8 μM, respectively (data not shown). This indicates that the concentration-dependent change in α-helical content at low temperatures occurs also at pH 8.0 and that there is no large secondary structural difference of F$_1$I at pH 8.0 compared to pH 6.7 in 20 mM KPB at 0.3 °C. In addition, melting curves were determined for three different concentrations of bmF$_1$I in 20 mM KPB (pH 8.0) (data not shown). The derived T_m was again concentration-dependent and measured 44.1, 48.0, and 50.9 °C for F$_1$I concentrations of 0.35, 0.8, and 1.8 μM, respectively. These melting temperatures are not significantly different from the ones obtained at pH 6.7 for comparable concentrations of F$_1$I.

However, when the CD melting curves were recorded at pH 8.0 in a buffer of higher ionic strength, such as 100 mM KPB, the CD signal was reduced and the thermal profile revealed a T_m of 44.6 and 51.3 °C for the 5 and 20 μM solution, respectively (data not shown). These values imply that interactions between F$_1$I molecules still exist, but overall the protein is less stable at this higher ionic strength.

The CD signal was also recorded for a 5 μM solution of F$_1$I in 100 mM KPB at pH 4.01 and 2 °C, and the θ_{222} value was found to be −12 100 deg cm^2 dmol^{-1}. This value indicates that F$_1$I contains considerably less α-helix and more random coil at pH 4.0. Again, a melting profile was determined for solutions of F$_1$I at concentrations of 5, 10, and 20 μM in 100 mM KPB at pH 4.01. As can be seen from Figure 8, the melting behavior at pH 4.0 is independent of the concentration of F$_1$I, indicating lack of structural stabilization by intermolecular interaction. These results further suggest that the structure of F$_1$I is unstable at pH 4.0 even at temperature as low as 2 °C. It should also be noted that lowering the pH to 4.0 causes a rapid loss of α-helical structure. Within 3 min of adjusting the pH to 4.0, the θ_{222} value increased to −12 100 deg cm^2 dmol^{-1} and remained for at least 30 min (data not shown).

The lack of structural stability at pH 4.0 might possibly be due to the following. Nearly 50% of the amino acid residues in F$_1$I are charged at physiological pH. The spacing of oppositely charged amino acid residues in the C-terminal 50 amino acid residues is such that it would allow the formation of α-helix-stabilizing salt bridges at neutral pH. At pH 4, aspartyl and glutamyl residues are most likely protonated, thus preventing the formation of these stabilizing intrahelical

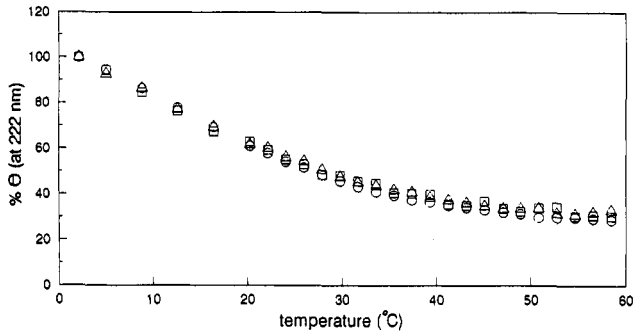

FIGURE 8: Thermal stability studies at pH 4.01 were performed for bmF_1I at a concentration of 5 (circles), 10 (squares), and 20 μM (triangles), respectively, in 100 mM KPB (see also Experimental Procedures). The plot shows the *F* value for increasing temperatures. The protein structure deteriorated rapidly as the temperature increased above 2 °C, and a T_m could not be determined. This loss of structure was independent of protein concentration.

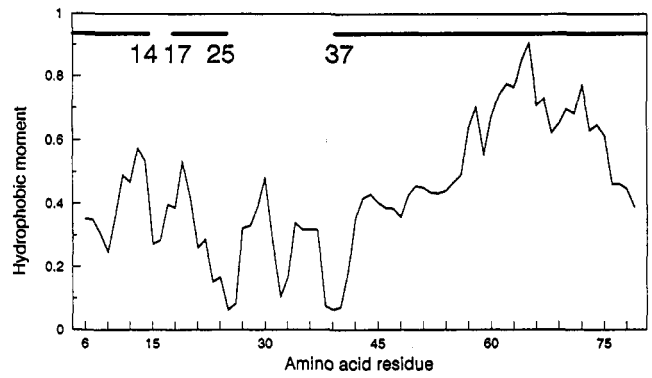

FIGURE 9: Hydrophobic moment analysis on the amino acid sequence of bmF_1I. The first region is considerably amphiphilic although the first two residues do not meet the criteria set by Parker and Song (1990).

ion pairs. Furthermore, the net positive charge of F_1I at pH 4.0 could be as high as 23 (if all aspartyl and glutamyl residues were protonated) versus a net positive charge ranging between +1 and +6 at pH 6.7, depending on the protonation of the histidyl residues. Electrostatic repulsions between F_1I molecules would further destabilize α-helix formation and intermolecular interaction at pH 4.0.

The loss of secondary structure at pH 4.0 is interesting in view of an earlier report (Panchenko & Vinogradov, 1985) where preincubation of F_1I at pH 4.8 resulted in a much faster inhibition of F_1-dependent ATP hydrolysis compared to a preincubation at pH 8.2.

The melting curves and the T_m for F_1I at pH 6.7 and 8.0 support the theoretically obtained prediction that F_1I forms a dimer or oligomer through coiled-coil interaction. Preliminary NMR data are consistent with this and suggest F_1I to be a dimer (Baleja, Van Heeke, and Schuster, unpublished observation). However, NMR data may be difficult to interpret F_1I especially with respect to physiological relevance. NMR experiments require that F_1I be at a high concentration, a condition which clearly affects the secondary structure as judged by CD analysis.

The CD experiments also demonstrate that at pH 8.0 the ionic strength of the F_1I solution greatly influences stability of the molecule.

While the manuscript for this paper was in revision, Lebowitz and Pedersen (1993) reported the expression of the rat liver F_1I from a cDNA clone in *E. coli*; the sequence of rat liver and bovine heart mitochondrial F_1I are highly homologous. They also performed a structural analysis by CD of their recombinant protein. Results from our structural analysis are consistent with their finding that F_1I is largely α-helical. Unfortunately, the exact secondary structural content cannot be directly compared as the concentration of F_1I and the ionic strength of the solution is vastly different in both studies. Lebowitz and Pedersen (1993) performed the CD analysis at a concentration of 63 μM F_1I in a high ionic strength buffer. On the basis of a change of the ratio $|\theta_{222}|/|\theta_{222}|$, they demonstrated a pH-dependent conformational change of F_1I in a pH range from 4.6 to 8.5. Where our results also indicate a sharp decrease in α-helical content for F_1I at pH 4.0, we did not detect a significant difference in secondary structure between F_1I at pH 6.7 and 8.0. From our data, the ratio of $|\theta_{222}|/|\theta_{222}|$ is calculated to be 1.143 and 1.149 for F_1I at 0.8 μM, 0.3 °C, and pH 6.7 and 8.0, respectively. This diverging conclusion could again be due to the different conditions of ionic strength and F_1I concentration. It should be noted that F_1I shows a maximum inhibitory activity *in vitro* at a concentration between 1 and 2 μM (see Figure 5), and this activity decreases rapidly as the concentration increases. This optimal concentration is hardly affected when the ionic strength of the assay buffer is varied between 19 and 176 mM (data not shown). Our results indicate a strong effect of protein concentration and ionic strength on the secondary structure and stability of F_1I and therefore suggest that conclusions drawn from CD studies performed on this protein at a concentration of 63 μM in high ionic strength buffer (Lebowitz & Pedersen, 1993) should be interpreted cautiously.

The F_1I amino acid sequence was further subjected to a hydrophobic moment analysis. It has been demonstrated that such an analysis is valuable to predict α-helical regions in predominantly α-helical proteins (Parker & Song, 1990; Bowie *et al.*, 1990). This theoretical analysis pedicts slightly less overall α-helical content in F_1I than was obtained from CD calculations. Figure 9 predicts that three amphiphilic helical segments can be distinguished in F_1I (shown by solid bars on top of the figure). When the hydrophobicity of the histidyl residues was set to +1.1 (noncharged species at, for instance, pH 8.0), the C-terminal helix could possibly extend N-terminally to residue 37 (see Figure 9). The assignment of this long α-helical stretch to the C-terminal portion of F_1I is in agreement with our statistical prediction of a coiled-coil structure for that region. A decrease of the pH from 8.0 to 6.7 would lead to a titration of histidyl residues, preferentially of those in a polar environment (the hydrophilic side of the coiled-coil). Titration of all histidyl residues would increase the net positive charge of F_1I from +1 to +6, thereby increasing the electrostatic repulsion between F_1I molecules. This repulsion might make certain amino acid side chains more accessible to interact with F_1 and cause inhibition of ATP hydrolysis.

Klein *et al.* (1982) have reported that bmF_1I has the tendency to form aggregates in aqueous solutions at low salt concentrations. Furthermore, cross-linking experiments have shown that F_1I can form a series of oligomers of up to a tetramer (Klein *et al.*, 1980; Couton and Van Heeke, unpublished observations). This oligomer formation was shown to be concentration- and pH-dependent with a minimal tendency to form oligomers at pH values between 6.5 and 7.0. Since the electrostatic repulsion is less at pH 8.0 vesus pH 6.7 and electrostatic interactions are reduced at elevated salt concentrations, aggregates might form more easily at higher pH and lower ionic strength. The formation of trimers and tetramers observed at higher concentrations and low ionic strength might explain the concentration dependence of the

CD signal and ionic strength dependence of the F$_1$I stability and the decrease in inhibitory activity of F$_1$I as its concentration is increased above 2 μM. Klein *et al.* (1982) also suggested earlier that oligomer formation may yield an inactive form of F$_1$I.

In summary, large quantities of recombinant bmF$_1$I have been expressed from a synthetic gene in *E. coli*. The protein was directed to the bacterial periplasmic space from which it was then easily purified in a rapid and single chromatographic step. The synthetic gene and its edited restriction enzyme site distribution will greatly facilitate future mutagenesis efforts. Recombinant bmF$_1$I was shown to be biologically active in that it inhibited both beef heart and *S. cerevisiae* mitochondrial F$_1$-ATPase with a pH sensitivity and turnover dependence characteristic of F$_1$I purified from beef heart mitochondria.

Thorough theoretical analysis of the primary structure of bmF$_1$I suggest that its C-terminal region is engaged in a coiled-coil structure. This prediction was experimentally supported by the results obtained from detailed CD studies. On the basis of these results, it is proposed that F$_1$I forms at least a dimer through coiled-coil interactions in the C-terminal part of the molecule. The structure of F$_1$I is furthermore very sensitive to the ionic strength of its solution, while both the structure and its activity are greatly affected by the concentration of F$_1$I. CD analysis did not reveal significant changes in secondary structure of F$_1$I at pH 6.7 compared to pH 8.0 (i.e., active versus inactive form of F$_1$I). However, pH-dependent changes in tertiary or quaternary structure would not necessarily be detected and thus cannot be ruled out as critical for conversion of the active to inactive form. Actual proof of the proposed coiled-coil structure of bmF$_1$I will have to await further detailed structural analyses.

ACKNOWLEDGMENT

The authors thank William P. Parker for stimulating discussions, Sandy Denslow, Todd Lowther, and Craig Banull for technical assistance during parts of this work, and Steve McClellan for production of the polyclonal antiserum.

REFERENCES

Baker, T. A., Grossman, A. D., & Gross, C. A. (1984) *Proc. Natl. Acad. Sci. U.S.A. 81*, 6779–6783.
Bowie, J. U., Reidhaar-Olson, J. F., Lim, W. A., & Sauer, R. T. (1990) *Science 247*, 1306–1310.
Chen, Y. H., Yang, J. T., & Chau, K. H. (1974) *Biochemistry 13*, 3350–3359.
Cintron, N. M., & Pedersen, P. L. (1979) *J. Biol. Chem. 254*, 3439–3443.
Cintron, N. M., Hullihen, J., Schwerzmann, K., & Pedersen, P. (1982) *Biochemistry 21*, 1878–1885.
de Boer, H. A., & Kastelein, R. A. (1986) *Maximizing Gene Expression* (Reznikoff, W., & Gold, L., Eds.) Butherworths Publishers, Stoneham, MA.
Dianoux, A.-C., & Hoppe, J. (1987) *Eur. J. Biochem. 163*, 155–160.
Ebel, R., & Lardy, H. (1975) *J. Biol. Chem. 250*, 191–196.
Ebner, E., & Maier, K. (1977) *J. Biol. Chem. 252*, 671–676.
Frangione, B. E., Rosenwasser, H. S., Penefsky, H. C., & Pullman, M. E. (1981) *Proc. Natl. Acad. Sci. U.S.A. 78*, 7403–7407.
Fujii, S., Hashimoto, T., Yoshida, Y., Miura, R., Yamano, T., & Tagawa, K. (1983) *J. Biochem. 93*, 189–196.
Ghrayeb, J., Kimura, H., Takahara, M., Hsiung, H., Masui, Y., & Inouye, M. (1984) *EMBO J. 3*, 2437–2442.
Goff, S. A., & Goldberg, A. L. (1985) *Cell 41*, 587–595.
Gruys, K. J., Urbauer, J. L., & Schuster, S. M. (1985) *J. Biol. Chem. 260*, 6533–6540.
Hanahan, D. (1983) *J. Mol. Biol. 166*, 557–580.
Harris, D. A., Von Tscharner, V., & Radda, G. (1979) *Biochim. Biophys. Acta 548*, 72–84.
Hashimoto, T., Negawa, Y., & Tagawa, K. (1981) *J. Biochem. 90*, 1151–1157.
Horstman, L., & Racker, E. (1973) *J. Biol. Chem. 245*, 1336–1344.
Husain, I., & Harris, D. A. (1983) *FEBS Lett. 160*, 110–114.
Kayalar, C., Rosing, J., & Boyer, P. D. (1977) *J. Biol. Chem. 252*, 2486–2491.
Klein, G., Satre, M., & Vignais, P. (1977) *FEBS Lett. 84*, 129–134.
Klein, G., Satre, M., Dianoux, A. C., & Vignais, P. V. (1980) *Biochemistry 19*, 2919–2925.
Klein, G., Satre, M., Dianoux, A. C., & Vignais, P. V. (1981) *Biochemistry 20*, 1339–1345.
Klein, G., Satre, M., Zaccai, G., & Vignais, P. V. (1982) *Biochim. Biophys. Acta 681*, 226–232.
Knowles, A. F., & Penefsky, H. C. (1972a) *J. Biol. Chem. 247*, 6617–6623.
Knowles, A. F., & Penefsky, H. C. (1972b) *J. Biol. Chem. 247*, 6624–6630.
Lebowitz, M. A., & Pedersen, P. L. (1993) *Arch. Biochem. Biophys. 301*, 64–70.
Lupas, A., Dyke, M. V., & Stock, J. (1991) *Science 252*, 1162–1164.
Manavalan, P., & Johnson, W. C. (1987) *Anal. Biochem. 167*, 76–85.
Matsubara, H., Hase, T., Hashimoto, T., & Tagawa, K. (1981) *J. Biochem. 90, 1159*–1165.
Milgrom, Y. (1991) *Eur. J. Biochem. 200*, 789–795.
Nelson, N., Nelson, H., & Racker, E. (1972) *J. Biol. Chem. 247*, 7657–7662.
Nieuwenhuis, F. J. R., Van De Drift, J. A. M., Voet, A. B., & Van Dam, K. (1974) *Biochim. Biophys. Acta 368*, 461–463.
O'Shea, E. K., Rutkowski, R., & Kim, P. S. (1989) *Science 243*, 538–542.
Panchenko, M., & Vinogradov, A. (1985) *FEBS Lett. 184*, 226–230.
Parker, W., & Song, P. S. (1990) *J. Biol. Chem. 265*, 17568–17575.
Pulman, M. E., & Monroy, G. C. (1963) *J. Biol. Chem. 238*, 3762–3769.
Rimm, D. L., & Pollard, T. D. (1989) *Gene 75*, 323–327.
Rouslin, W. (1991) *J. Bioenerg. Biomembr. 23*, 873–888.
Sambrook, J., Fritsch, E. F., & Maniatis, T. (1989) *Molecular Cloning, A Laboratory Manual*, Cold Spring Harbor Laboratory, Cold Spring Harbor, NY.
Schagger, H., & von Jagow, G. (1987) *Anal. Biochem. 166*, 368–379.
Schwerzmann, K., & Pedersen, P. L. (1981) *Biochemistry 20*, 6305–6311.
Schwerzmann, K., & Pedersen, P. L. (1986) *Arch. Biochem. Biophys. 250*, 1–18.
Sheng, S., Moraga, D. A., Van Heeke, G., & Schuster, S. M. (1992) *Protein Expression Purif. 3*, 337–346.
Smith, J. B., & Sternweis, P. C. (1977) *Biochemistry 16*, 306–311.
Studier, F. W., Rosenberg, A. H., Dunn, J. J., & Dubendorff, J. W. (1990) *Methods Enzymol. 185*, 60–88.
Van de Stadt, R., DeBoer, B., & Van Dam, K. (1973) *Biochem. Biophys. Acta 292*, 338–349.
Van Heeke, G., Shaw, R., Schnizer, R., Couton, J. M., Schuster, S. M., & Wagner, F. W. (1993) *Protein Expression Purif.* (in press).
Von Heijne, G. (1983) *Eur. J. Biochem. 133*, 17–21.
Walker, J. E., Gay, N. J., Powell, S. J., Kostina, M., & Dyer, M. R. (1987) *Biochemistry 26*, 8613–8619.
Wong, S.-Y., Galante, Y. M., & Hatefi, Y. (1982) *Biochemistry 21*, 5781–5787.